Hindawi Publishing Corporation
Journal of Electrical and Computer Engineering
Volume 2010, Article ID 840895, 9 pages
doi:10.1155/2010/840895

Research Article

Channel Characterization for 700 MHz DSRC Vehicular Communication

Raffi Sevlian,[1] Carl Chun,[1] Ian Tan,[1] Ahmad Bahai,[1] and Ken Laberteaux[2]

[1] *Department of Electrical Engineering and Computer Sciences, University of California, Berkeley, Berkeley, CA 94720, USA*
[2] *Toyota Technical Center, Ann Arbor, MI 48105, USA*

Correspondence should be addressed to Raffi Sevlian, raffisev@gmail.com

Received 19 March 2010; Accepted 5 July 2010

Academic Editor: C. C. Jay Kuo

Copyright © 2010 Raffi Sevlian et al. This is an open access article distributed under the Creative Commons Attribution License, which permits unrestricted use, distribution, and reproduction in any medium, provided the original work is properly cited.

Adapting OFDM for vehicular communication requires extensive knowledge of anticipated multipath and Doppler environments. We present a GPS-enabled channel sounding system built and used to conduct a channel measurement campaign. Tests conducted at the 700 MHz band in and around downtown Ann Arbor, Michigan, explored various vehicle-to-vehicle and vehicle-to-roadside channel scenarios. The measured channel metrics are used to quantify the effects on guard interval, packet duration, and subcarrier spacing for a functional OFDM system at 700 MHz. This paper is one of the first to present vehicular-based channel-modeling results from measured data in the 700 MHz band.

1. Introduction

The past half century has seen a monumental growth in the world's transportation infrastructure. Almost all of this investment has come in the form of new roads and other large earthworks. With the rapid miniaturization of electronics and advancements in computing and communications technology, there has been heavy interest by governments in intelligent transportation systems (ITS) [1]. Intelligent transportation promises the convergence of modern information technology (IT), communication infrastructure, and sensing technology with standard transportation systems to improve safety, reduce transportation times, minimize vehicle wear, and optimize fuel consumption.

Many specific examples of ITS have been proposed and are currently in phases of testing or deployment. Applications range from vehicle-based collision avoidance to general traffic monitoring and toll collection. Common to all these applications is a need for a very robust communication system [2]. Dedicated short range communication (DSRC) encompasses all such vehicle-to-vehicle (V2V) or vehicle-to-roadside (V2R) communication.

1.1. 5.9 GHz DSRC. The 802.11p standard is a proposed amendment to 802.11 that governs 5.9 GHz vehicular communication [3]. It borrows heavily from the 802.11a standard. IEEE 802.11a uses a 20 MHz bandwidth signal with two separate frequency regions of 5.17–5.23 GHz and 5.735–5.835 GHz. In IEEE 802.11p, transmissions employ a 10 MHz bandwidth OFDM signal at 5.85–5.925 GHz. Both standards use 52 subcarriers, so while 802.11a has a subcarrier spacing of 312.5 kHz, 802.11p has a subcarrier spacing of 156.25 kHz. To help compensate for the outdoor mobile environment, 802.11p specifies longer guard intervals, training sequences, and preambles.

1.2. 700 MHz DSRC. In addition, the 5.9 GHz band allocated for DSRC, there is new interest in vehicular-based communications in the 700 MHz band. The initial push into this frequency was done by the Japanese Transportation Institute in an effort to develop a new DSRC-like communication system. Also, the FCC has recently explored the use of unused 700 MHz spectrum for white space applications. These are unlicensed applications that actively avoid interference with licensed applications in the same band.

The 700 MHz frequency band offers a significant coverage advantage over current 5.9 GHz DSRC implementations. At an identical transmitter power, a low-frequency signal will have greater range than a high-frequency signal due to

decreased free space attenuation and lower absorption by various building materials and obstructions.

Since a properly designed OFDM scheme has high immunity to multipath [4], the 700 MHz band offers potential for low-complexity, low-power OFDM transceivers. Currently, there is no standard defined for DSRC communication in the 700 MHz band. Most likely, the proposed technology for such a standard will be an 802.11-type OFDM scheme. In order for a proper scheme to be developed, the wireless channel at 700 MHz must be understood, and channel models for various environments must be determined.

2. Previous Work

There has been substantial research in the 2.4 GHz and 5.9 GHz vehicular channels which provide a solid framework for our 700 MHz investigation. Acosta et al. reported doubly selective models of an expressway at 2.4 GHz [5] and 5.9 GHz [6] and provided analysis of the Doppler and multipath characteristics. Zhao et al. conducted extensive urban and suburban measurements at 5.3 GHz to capture delay spread [7] and Doppler [8] statistics. Cheng et al. used 5.9 GHz empirical models [9] to study the performance of scaled channel bandwidths in mobile vehicle-to-vehicle situations [10]. Both Zhao [7] and Tan [11] related 5.9 GHz channel metrics to their effects upon DSRC OFDM performance.

Although there has not been specific empirical research at 700 MHz, some early work examined outdoor channel characteristics at 900 MHz [12, 13]. However, these works do not cover the environments that a robust vehicular DSRC system would encounter. Cox [12] only examines the infrastructure to vehicle scenario and only at slow speeds of less than 5 miles per hour. The results presented in [13] are limited to the path loss and delay spread of stationary scenarios.

With the opening of the 700 MHz spectrum, there is a great need to thoroughly investigate and understand communications at these frequencies. This research is one of the first to present vehicular-based channel modeling results from measured data in this band.

In this paper, we present the results of field tests that determine channel statistics for a variety of scenarios. Our probing signal was 6 MHz in bandwidth and centered at 794 MHz. Tests were conducted in urban and highway environments under realistic, uncontrolled traffic conditions. Delay and Doppler statistics are calculated to determine the impairments caused by the channel and to examine their influence upon the OFDM system. The presented results provide insight into OFDM design for white space applications in the public safety domain or for highly mobile outdoor devices.

3. Wireless Channel Model

The wireless channel is typically modeled as a stochastic, linear, time-varying system. This model is a good representation of a vehicular channel due to the constant movement and evolution of signal scatters in the wireless environment.

Analytically, the wireless channel may be defined as a set containing a finite number of time-varying multipath components [14, 15]. The impulse response and frequency response are described by (1) and (2), respectively,

$$h(\tau, t) = \sum_i a_i(t)\delta(\tau - \tau_i(t)), \tag{1}$$

$$H(f; t) = \sum_i a_i(t)e^{-j2\pi f \tau_i(t)}. \tag{2}$$

To effectively characterize such systems, we utilize certain channel metrics that are computed from the time-varying impulse response. Typically, the baseband sampled version of the impulse response is used for metric calculations. We denote $h_b[m, n]$ as a baseband channel's discrete equivalent to the analog passband channel $h(\tau, t)$. These relationships are discussed in detail within [14].

A deterministic, time-domain model is used in our analysis. Each time-varying impulse response is converted into a power delay profile (PDP). The channel is averaged over a period of time to calculate the number and severity of reflections produced by the environment. These provide multipath metrics useful in OFDM design. Time-varying characteristics are measured by coherence time and Doppler spread statistics.

4. Multipath Metrics

4.1. PDP Metrics. The power delay profile (PDP) is related to the baseband discrete channel impulse response by

$$h_{\text{PDP}}[p] = \frac{1}{N_f} \sum_{k=0}^{N_f - 1} |h_b[p, Lk]|^2. \tag{3}$$

The averaging technique in (3) averages $h_b[m, n]$ for each multipath tap over the number of impulse responses. L is the length of each impulse response and N_f is the number of impulse responses that are averaged. This quantity depends upon the impulse responses contained within each data capture. N_f is constant throughout our analyses, as our data capture sizes for each test are identical.

This generates a PDP which quantifies the number and severity of echoes in the wireless channel. The PDP is used to calculate various multipath statistics such as mean excess delay, root mean square (RMS) delay, and max excess delay. The various statistics described are illustrated in Figure 1.

Mean excess delay, T_{MEAN}, is the first moment of the PDP and represents the delay of the typical echo,

$$T_{\text{MEAN}} = \frac{\sum_p |h_{\text{PDP}}[p]|\, p}{\sum_p |h_{\text{PDP}}[p]|}. \tag{4}$$

The RMS delay spread, T_{RMS}, is the second moment of the PDP and quantifies the spread of the echoes in time

$$T_{\text{RMS}} = \sqrt{\overline{T^2} - (T_{\text{MEAN}})^2}, \tag{5}$$

$$\overline{T^2} = \frac{\sum_p |h_{\text{PDP}}[p]|\, p^2}{\sum_p |h_{\text{PDP}}[p]|}. \tag{6}$$

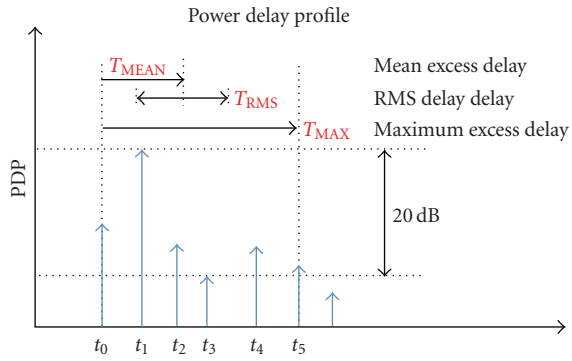

Figure 1: PDP and measured delay statistics.

The maximum excess delay, T_{MAX}, defines the time between the first and last detectable echo in the channel. For practical considerations, detectable is defined as some threshold power level below the maximum power level. In most situations, only components within 20 dB below the strongest detectable multipath are considered.

4.2. Coherence Time. For a time-varying impulse response, a coherence time can be defined as the length of time for which the impulse response is considered time invariant. The time domain autocorrelation for each impulse response at lag k is calculated from the baseband response, $h_b[m,n]$,

$$R_{hh}[m,k] \approx \sum_{n=0}^{N_f-1} h_b[m,n]h_b^*[m,n+k], \tag{7}$$

N_f is the number of estimated impulse responses in a given data capture. In our measurements, N_f was 1446. From $R_{hh}[m,k]$ in (7), the coherence time of each tap, $T_c[m]$, is defined as the autocorrelation lag for which $R_{hh}[m,k]$ is half of its maximum value (which occurs when $k = 0$)

$$R_{hh}[m, T_{c(50)}] = \frac{R_{hh}[m,0]}{2}. \tag{8}$$

The coherence time of the channel is the weighted average coherence time of each tap. The weights are determined by the average power of each channel tap.

4.3. Doppler Spread. The Doppler spectra of a channel quantifies the frequency spreading caused by a time-varying channel. It is defined as the Fourier transform of the time domain autocorrelation function (9) or the power spectral density (PSD) of each time-varying channel tap

$$S_{HH}(m,\nu) = \sum_{n=-\infty}^{n=\infty} R_{hh}[m,k]e^{-2\pi\nu k}. \tag{9}$$

For a channel with a fixed transmitter and moving receiver, the Doppler spread, D_s, can be calculated, assuming a uniform angle of arrival, by the following:

$$D_s = \frac{2f_c v_{\text{rel}}}{c}, \tag{10}$$

where f_c is the carrier frequency, v_{rel} is the relative velocity of the receiver and transmitter and c is the speed of light.

When both the transmitter and receiver are in motion, the Doppler spectrum follows a "two-ring model" [16]. The Doppler spread in this situation can be shown to be defined as

$$D_s = \frac{K f_c}{c\sqrt{2}}\sqrt{v_{tx}^2 + v_{rx}^2}, \tag{11}$$

where K is some constant determined empirically. The variables v_{tx} and v_{rx} are the velocity of the transmitter and receiver, respectively.

The Doppler spread is calculated by the RMS spread of the Doppler spectrum for each tap. The Doppler spread of the channel is the weighted average of each tap's Doppler spread. The weights are determined by the average power of each each channel tap.

It can be shown that under uniform angle of arrival, the Doppler spread is inversely related to the coherence time of the channel. This relation is often used to estimate one relation from the other. However, we choose to rely on the formal definitions in (9) and (7), since they are not based on any assumptions of ideal channel behavior.

4.4. Coherence Bandwidth. By looking at the frequency response of the wireless channel at any moment in time, we can determine the flatness of the channel. This flatness is used to determine whether a transmitted signal is undergoing frequency selective or flat fading. In frequency selective fading, the transmitted signal is relatively wide compared to the average width of ripples in the channel's frequency response. Therefore, different frequency components of the signal will undergo different channel gains. In flat fading, the channel response is flat over the frequency band of interest, so the entire signal effectively experiences the same gain.

A coherence bandwidth is used to quantify the frequency range for which the channel response can be considered flat. Given the frequency response of the channel,

$$H(f;t) = \sum_i a_i(t)e^{-j2\pi f\tau_i(t)}, \tag{12}$$

an autocorrelation function $R(\delta;t)$ can be defined from $H(f,t)$ as follows:

$$R_{HH}(\delta;t) = \frac{E[H(f;t)H^*(f+\delta;t)]}{E[H(f;t)H^*(f;t)]}. \tag{13}$$

From the autocorrelation, $R_{HH}(\delta)$, with t held constant, we define the coherence bandwidth as the value of δ for which $R_{HH}(\delta)$ is 50% of its maximum value $R_{HH}(\delta = 0)$. This is considered the 50% coherence bandwidth ($B_{c(50)}$).

It can be shown that the coherence bandwidth is inversely related to the RMS delay of the channel [15]. The 50% coherence bandwidth is approximated by

$$B_{c(50)} \approx \frac{1}{2\pi T_{\text{RMS}}}. \tag{14}$$

5. Channel Sounding Methodology

A pulse-compression technique was used to determine the baseband discrete channel impulse response. Previous work [6, 11, 12] show the usefulness of such techniques in broadband characterization. For this technique, a pseudo-random noise symbol sequence is transmitted over the air and recovered at the receiver. This technique leverages the transmit signal's impulse-like autocorrelation.

5.1. Channel Sounding Hardware. The 700 MHz channel sounding system consists of a transmitter and receiver installed in separate vehicles. The transmitter consists of a laptop, differential GPS (DGPS) unit, Aeroflex 3416 signal generator, high power amplifier, and a 0 dBi MaxRad roof-mounted, omnidirectional antenna. During operation, the laptop and DGPS continually record the transmitter's location while the signal generator transmits the sounding signal. The 700 MHz receiver consists of a laptop, differential GPS unit, Tektronix 6106A real-time signal analyzer (RSA), a 32 dB LNA, and a roof-mounted MaxRad omnidirectional antenna.

For 700 MHz testing, the data portion of the sounding signal is 511 symbols in length and generated at a symbol rate of 6 Msym/s, yielding a time resolution of 166.7 ns. By constructing a null period of equal length following each data transmission, the signal may detect maximum excess delays up to 85.17 μs in length. Since delay spreads are expected to be no more than a few microseconds in length, this provides sufficient delay spread resolution. Each frame is 170.3 μs long, leading to a repetition rate of 5.87 kHz. This allows Doppler spreads ranging between $\pm$2.935 kHz to be unambiguously measured with a resolution of approximately 4 Hz.

6. Measured Channel Metrics

Various channel sounding tests were performed in and around downtown Ann Arbor, Michigan. These field tests were performed under a variety of realistic DSRC channel environments. This research classifies the environments as either urban or highway and possible situations as line-of-sight (LOS) or non-line-of-sight (NLOS). Measurements were captured in normal driving conditions, resulting in data from a variety of distances and velocities.

Due to FCC regulations, experimental transmissions could not interfere with licensed television broadcasting in the area. In order to avoid occupied spectrum at the testing sites, the tests were conducted with a 6 MHz bandwidth signal centered at 794 MHz. This spectrum was unoccupied in all the testing locations and FCC approval was obtained for the tests performed.

The highway measurements were taken along the highways that border Ann Arbor, Michigan. The highways consists of state route M-14 to the north, Interstate 94 to the south and west, and highway US-23 to the east. Most of the LOS measurements were taken along M-14 and US-23. The NLOS situations on the highway utilized large semi-trailer trucks acting as blockers and occurred primarily along I-94. Measurements were conducted in light to moderate traffic with speeds consistently above 45 miles per hour.

Table 1: Channel scenario RX/TX separation [meters].

	Highway		Urban	
Scenario	LOS	NLOS	LOS	NLOS
25 p.	9	120	68	121
50 p.	67	164	154	163
75 p.	124	229	354	293

Urban measurements were taken in several locations: a mall, downtown, and along an urban strip. One test site was the Arborland Mall which consisted of a parking lot and a ring of one- and two-story businesses. Measurements were also taken in a downtown business area which was bordered by 3rd Street to the west, West Huron Street to the north, 5th Avenue to the east, and West William Street to the south. The long straight stretch of State Street between East Liberty Street and East Madison Street provided a location for long LOS measurements. Most LOS measurements were taken along State Street with traffic between the two vehicles. Most of the NLOS measurements were captured in the Arborland Mall and downtown area. Speeds of the vehicles depended on the traffic conditions and ranged from stopped to 35 miles per hour.

The experiments reported here were done in real-world traffic where all variables could not be controlled by the authors. Therefore, we were not capable of repeating a specific experiment multiple times to adjust individual parameters, such as RX/TX separation. Consequently, any trends relating to vehicle separation are difficult to infer, since sample size, both for any given distance and across wide ranges of distances, are small. The efficacy of our measurements lie in their grounding in reality; these are scenarios and situations that communication systems engineers will face when designing vehicular wireless infrastructures. For completeness, Table 1 presents the quartiles of separations encountered in the experiments to give further insight on the ranges encountered.

In the following sections, we discuss the results of our extensive trials in urban LOS and NLOS scenarios in and around downtown Ann Arbor, as well as various highway LOS/NLOS scenarios. The results are grouped by metric in the sections below. Using the methods outlined earlier, the PDP metrics are calculated and presented for various scenarios. General trends in these results are highlighted and discussed.

6.1. Mean Excess Delay. Using the formula outlined in (4), the mean excess delay is calculated for each scenario with results shown in Figure 2. The delays are presented as box plots as a function of testing environment. The box plots used to present the data in this report have lines at the lower quartile (25%), median (centerline), and upper quartile (75%) values. The whiskers are lines extending from each end of the boxes to show the maximum and minimum values

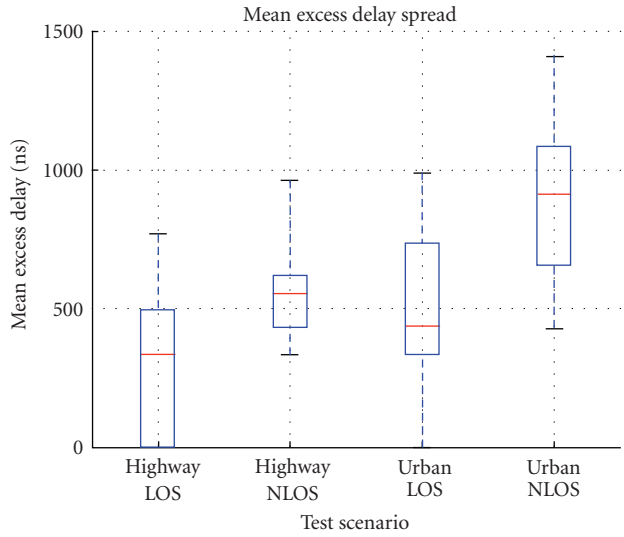

Figure 2: Comparison of mean excess delay for various scenarios.

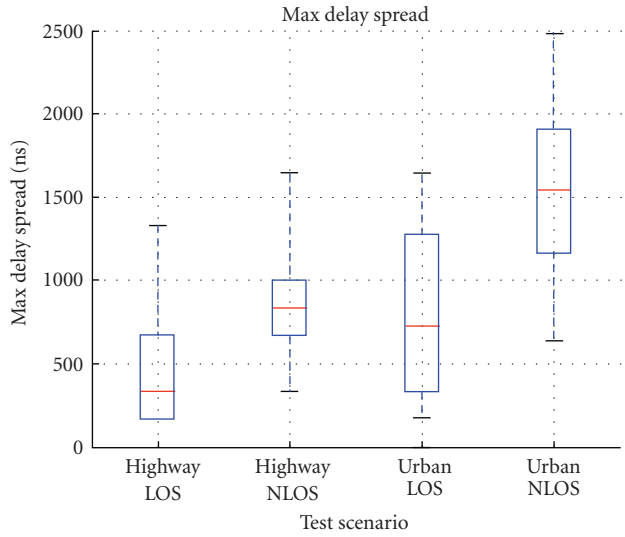

Figure 3: Comparison of maximum excess delay for various scenarios.

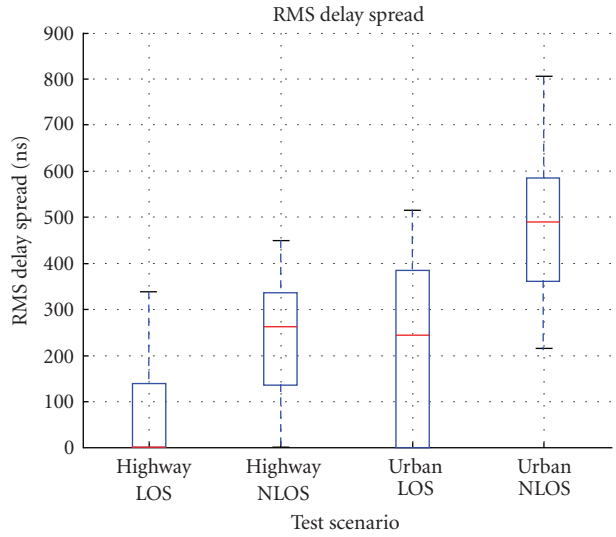

Figure 4: Comparison of RMS delay spread for various scenarios.

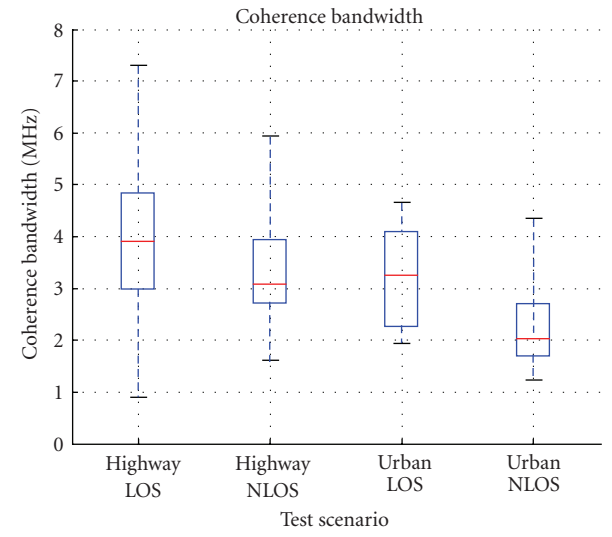

Figure 5: Comparison of coherence bandwidth for various scenarios.

of individual data captures. Therefore, there will be some outliers reported at these extremes.

The NLOS scenarios have much higher mean excess delay than LOS scenarios as the strong LOS component tends to dominate the PDP. In addition, transmitted signals in NLOS environments will encounter many different reflections along its path to the receiver. The urban NLOS shows the highest mean delay because many of the tests were done where the transmitter and receiver were blocked by multiple buildings. In the Highway NLOS scenarios, the transmitter and receiver line-of-sight was obstructed by only a few vehicles, and reflections also came from the walls on either side of the highway.

6.2. Maximum Excess Delay. In Figure 3, the max excess delay, as defined in Section 4.1, is shown for different scenarios. Data from the four situations of highway LOS, urban LOS, highway NLOS, and urban NLOS are presented. Max delay statistics are higher in the NLOS situations with median values consistently higher than their LOS counterparts.

Much like mean excess delay, urban NLOS has the highest reported maximum delay. This occurs again because of the many obstructions that the transmitted signal will encounter in and around a dense urban area.

6.3. RMS Delay Spread and Coherence Bandwidth. Using the definition provided in (5), the RMS delay spread is derived for various scenarios. The urban NLOS environment presents the most difficult multipath channel with observed delay spreads close to 1 μs.

Applying the approximate relation between coherence bandwidth and RMS delay spread in (14), the coherence bandwidth for various situations was calculated. The results are presented in Figure 5. The highway and urban NLOS

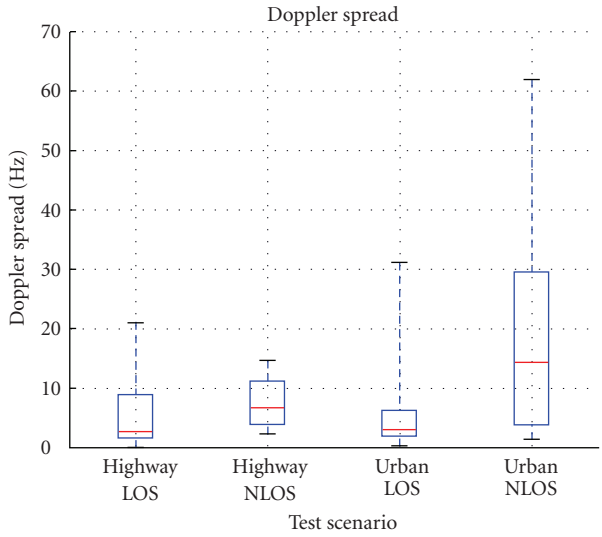

Figure 6: Comparison of Doppler spread for various scenarios.

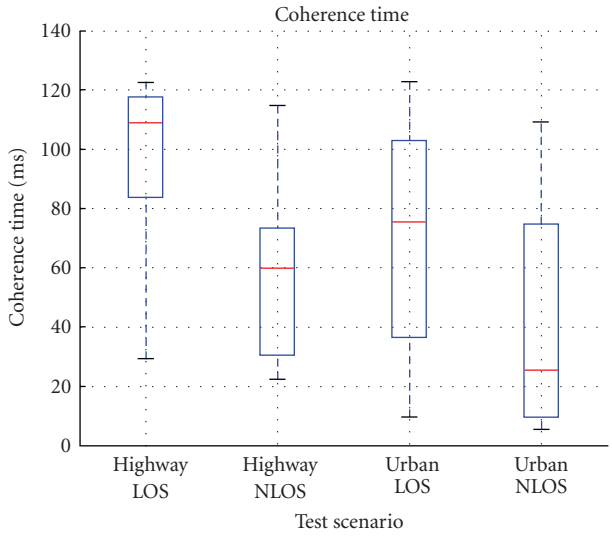

Figure 7: Comparison of coherence times for various scenarios.

scenarios have the lowest median coherence bandwidth of 3 MHz and 2 MHz, respectively.

High RMS delay is caused by a large number of reflections, of varying length, in the multipath environment. In an environment with high RMS delay, consecutive symbols will interfere with each other. This is an impairment known as inter-symbol interference, or ISI. For OFDM systems, this channel parameter affects the guard interval that is used to mitigate ISI. Since the urban NLOS environment lead to the highest multipath, it is the driving scenario for OFDM guard interval design.

Strong multipath environments also lead to small coherence bandwidths. This will affect the OFDM pilot spacing. As before, the strong multipath characteristic of urban environments lead to the most degraded and lowest bandwidth channels.

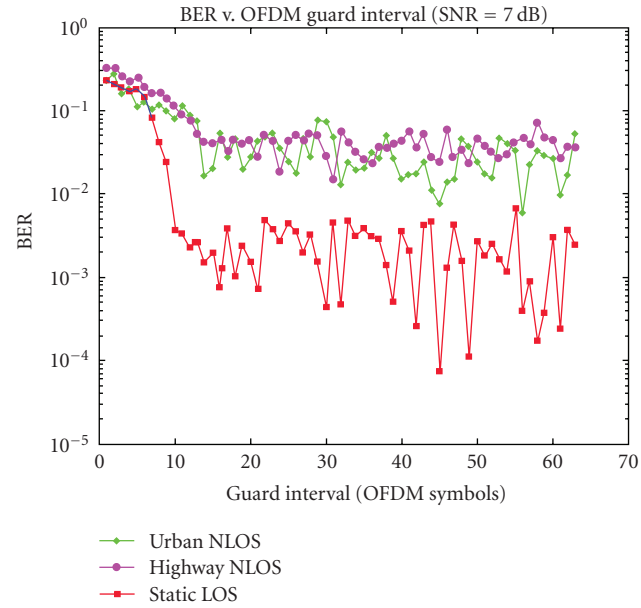

Figure 8: BER simulation of BPSK 1/2 rate with three channel models.

6.4. Doppler Spread. Figure 6 shows the measured Doppler spreads in a variety of scenarios. Urban NLOS has the highest median and reported Doppler spread. As noted earlier, the Doppler spread is caused by multiple angles of arrival and motion of the receiver and transmitter. Therefore, it is not surprising that both highway and urban NLOS environments will have considerable Doppler spread. Urban environments have low speed but have multiple angles of arrival for the receive signal. Highway environments have lower angular spread of the receive signal, but are at much higher velocities. In fact, in the highway LOS tests, the relative velocities are close to zero, yet the doppler spread is quite high. This supports modeling with the two ring model in (11).

6.5. Coherence Time. Coherence time measures the time that the channel can be considered time invariant. This will affect the duration of the packet if a single equalization is used in the beginning of each packet.

Coherence times were computed using the formula described in (7) and (8). Figure 7 presents a summary of coherence time for various situations. The shortest coherence times encountered are on the order of 1-2 ms.

7. OFDM System Design

Transitioning wireless communications from 5.9 GHz to 700 MHz requires a reexamination of the assumptions regarding the wireless channel. Transmission at lower frequencies will exhibit less attenuation in free space and urban environments. Less attenuation of the transmitted signal will lead to stronger reflections and thereby an increase in the observed delay spreads. At the same speed, lower communication frequencies will also lead to lower Doppler

Table 2: 700 MHz channel metrics.

Quartile/Extrema	T_{Mean} [ns]	T_{RMS} [ns]	T_{MAX} [ns]	T_{SDS} [ns]	D_S [Hz]	T_C [ns]	B_C [MHz]
min	0	0	166.667	0	1.49996	2.38467	1.063
25 p.	437.012	218.438	666.667	655.45	2.005	14.459	2.705
50 p.	672.753	368.666	1166.67	1041.419	12.00	42.5833	4.817
75 p.	971.283	523.992	1666.67	1495.275	23.99	82.3562	5.946
max	1454.88	815.446	2533.33	2270.326	62.02	124.343	7.212

Table 3: OFDM System design parameters.

Channel metric	OFDM system parameter constraint
Max Delay Spread ($T_{\max}$)	$T_{\max} <$ *OFDM* Guard Interval
Coherence Bandwidth ($B_{c(50)}$)	$B_c >$ *Subcarrier Spacing*
Doppler Spread (D_s)	$D_s <$ 10% Subcarrier Spacing
Coherence Time ($T_{c(50)}$)	$T_c >$ *Packet Duration*

Table 4: OFDM simulation parameters.

Simulation Parameter	Value
Modulation	BPSK
Channel Coding	1/2 rate convolutional coding
Channel Bandwidth	10 MHz
Subcarriers (N_{FFT})	64
Data Subcarriers	48
OFDM Subcarrier Spacing	156.25 kHz
OFDM Symbol time	100 ns (8 μs for 80 symbols)
Guard interval (CP)	5–64 OFDM Symbols

spreads and greater coherence times. These differences must be accounted for in the system design.

Table 2 summarizes the major metrics calculated for the 700 MHz channel. The data incorporates all the tested scenarios. The influence of these metrics upon OFDM system design must be examined to maximize performance. This investigation examines the effect of multipath delay, Doppler spread, coherence bandwidth, and coherence time at 700 MHz. The design requirements and their relation to channel metrics are shown in Table 3.

For OFDM channel equalization to work properly, the cyclic prefix length should be longer than the expected maximum delay of the channel. To quantify channel delay, the sum delay spread (T_{SDS}) is the sum of the mean delay and RMS delay spread and is an appropriate lower bound for the cyclic prefix length [11]. Because the channel delay is much greater in the 700 MHz environment than in 802.11a and 802.11p, the choice of guard interval duration must be reexamined. The channel models for 802.11a assume RMS delay spreads of 250 ns in the worst case NLOS case [17] and calls for a 800 ns guard interval. If the 802.11p guard interval is applied at 700 MHz, we see that it is insufficient protection in some situations. From the data in Table 2, the upper quartile of T_{MAX} and T_{SDS} exceeds 1.4 μs. Therefore, the guard interval will need to be longer than that specified for 802.11p to combat the increased likelihood of ISI at 700 MHz. Optimization for reliability of the safety messages would determine the necessary margin for ISI and the desired guard interval. We conclude that the OFDM guard interval must be increased beyond 1.4 μs.

The coherence bandwidth provides an upper bound on the allowable subcarrier spacing. In OFDM equalization, an initial channel response is estimated by the training sequence transmitted at the beginning of the packet. This produces a set of channel estimates for each subcarrier. For the estimated channel response for the entire band to be accurate, the channel response should be relatively smooth between each subcarrier. Therefore, the coherence bandwidth should be wider than the subcarrier spacing. The smallest reported coherence bandwidth which corresponds to the extreme NLOS scenarios was 1.063 MHz. The subcarrier spacing in 802.11p is 156.25 kHz. Therefore, channel response will be fairly smooth between each sample. The observed coherence bandwidth of the 700 MHz channel is not a limiting factor for an OFDM system based upon 802.11p.

Doppler spread provides a lower bound on the allowable subcarrier spacing. If the Doppler spread is high, individual subcarriers will "smear" onto each other and will no longer be orthogonal. A good rule of thumb is that Doppler spread should be less than 10% of the subcarrier spacing to prevent inter-carrier interference. The 700 MHz band has a much smaller Doppler spread than the 5.9 GHz band. The decrease in Doppler spread allows a future OFDM implementation the freedom of using many more subcarriers than 802.11a or 802.11p. In OFDM systems, subcarrier spacing must be at least 10–20 times greater than the Doppler spread of the channel. In the 700 MHz case, maximum Doppler spreads of 60 Hz correspond to a minimum subcarrier spacing of 0.6 kHz. The 802.11p baseband uses a subcarrier spacing of 156.25 kHz. Thus Doppler spread, like coherence bandwidth, should not limit a 700 MHz OFDM system based on 802.11p.

Coherence time affects the maximum length of the transmitted packet. The estimated channel response calculated at the beginning of the packet is effective only as long as the channel is constant during the packet. Therefore, the estimate is useful for as long as the coherence time unless more complex equalization schemes are used. At 5.9 GHz, extreme NLOS scenarios have coherence times on the order of 1 ms [11]. However, in the 700 MHz band, the reported coherence times are much larger. The median coherence times for urban NLOS scenarios is 20 ms, with the shortest time being 2 ms. At 5.9 GHz, assuming a 3 Mbps transmission rate, any packet over 367 bytes will experience multiple channel fades assuming a 1 ms coherence time

Table 5: OFDM simulation parameters.

Channel Type	T_{MEAN} [ns]	T_{RMS} [ns]	T_{MAX} [ns]	T_{SDS} [ns]	Doppler spread [Hz]
Static LOS	161.91	166.6	328.51	333.34	8
Highway NLOS	429.59	330.58	760.17	833.35	20
Urban NLOS	1125.3	559.95	1685.3	1833.4	30

[11]. At 700 MHz, assuming coherence times on the order 20 ms and a transmission rate of 3 Mbps, any packet over 7.2 kB will experience multiple channel fades. Therefore, a future system can increase the packet size bounds from the previous 802.11p sizing guidelines. However, it is important to note that the lowest coherence times occur in high speed NLOS environments where safety is in fact most crucial.

7.1. OFDM Baseband Simulations. Using a Simulink platform, we evaluate the performance of a 700 MHz OFDM system in a variety of measured channels. From the measured statistics, it has been shown that ISI at 700 MHz is a serious concern. Since the increase in ISI is most easily mitigated with an increased cyclic prefix, we examine the effect of guard interval length and bit error rate (BER).

We simulated the baseband OFDM according to the DSRC standard in [3]. A randomly generated symbol sequence with 1/2 rate convolutional code and BPSK is used. The simulations used the standard 48 OFDM data symbols with 4 symbols used for pilots. The simulations tested cyclic prefix lengths ranging from 10 symbols (1 μs) to the maximum of 64 symbols (6.4 μs). The OFDM parameters used in the simulation are shown in Table 4. A flat fading Rayleigh channel was assumed with 3 different channel (PDP) characteristics. The first model is a simple static line of sight with low Doppler spread. The second is a typical highway NLOS scenario with medium multipath and high Doppler spread. The third channel is a typical urban NLOS scenario with high multipath and medium Doppler spread. The channel statistics of these channel models are shown in Table 5.

The BERs of three channels plotted as a function of guard interval are shown in Figure 8. Each symbol has a 100 ns duration. From this simulation, it can be seen that the NLOS channels with large delay spreads require a guard interval at least as large as T_{SDS} to reach their lowest BER. As stated earlier from channel metric analysis, the current DSRC standard will work poorly in urban environments with considerable NLOS. The simulations confirm our assertion.

8. Conclusion

This investigation presents the results of an extensive campaign characterizing the mobile V2V and V2R channel at 700 MHz. Measurements reflected realistic driving scenarios including urban and highway environments at a variety of speeds and distances. This campaign is the first published set of measured delay and Doppler data for vehicular communications in the 700 MHz spectrum.

The delay and Doppler channel metrics derived from the measured data are used to determine the necessary parameters of an OFDM-based DSRC system at 700 MHz. The measured Doppler spread is much smaller than at 5.9 GHz and will not contribute to intercarrier interference. Coherence times at 700 MHz are longer than those observed for 802.11p and are more tolerant of increased packet lengths. Because of the large delay spreads measured in extreme NLOS situations, there is an increased susceptibility to ISI in the 700 MHz spectrum. Using the 5.9 GHz DSRC as a template, OFDM simulations showed the effect of guard interval length upon BER in several vehicular channels. Based upon the results presented, it has been shown that assumptions for 802.11p communications are not always applicable to the 700 MHz spectrum and any future system design must be adjusted accordingly.

References

[1] P. Varaiya, "Smart cars on smart roads. Problems of control," *IEEE Transactions on Automatic Control*, vol. 38, no. 2, pp. 195–207, 1993.

[2] D. Jiang, V. Taliwal, A. Meier, W. Holfelder, and R. Herrtwich, "Design of 5.9 GHz DSRC-based vehicular safety communication," *IEEE Wireless Communications*, vol. 13, no. 5, pp. 36–43, 2006.

[3] "Standard Specification for Telecommunications and Information Exchange Between Roadside and Vehicle Systems–5 GHz Band Dedicated Short Range Communications (DSRC) Medium Access Control (MAC) and Physical Layer (PHY) Specifications," ASTM Std. E2213-03, 2003, http://www.astm.org/.

[4] H. Schulze and C. Luders, *Theory and Applications of OFDM and CDMA: Wideband Wireless Communications*, Wiley, New York, NY, USA, 1st edition, 2005.

[5] G. Acosta and M. A. Ingram, "Model development for the wideband expressway vehicle-to-vehicle 2.4 GHz channel," in *Proceedings of IEEE Wireless Communications and Networking Conference (WCNC '06)*, pp. 1283–1288, April 2006.

[6] G. Acosta and M. A. Ingram, "Doubly selective vehicle-to-vehicle channel measurements and modeling at 5.9 GHz," in *Proceedings of the Wireless Personal Multimedia Communications Conference (WPMCC '06)*, September 2006.

[7] X. Zhao, J. Kivinen, P. Vainikainen, and K. Skog, "Propagation characteristics for wideband outdoor mobile communications at 5.3 Ghz," *IEEE Journal on Selected Areas in Communications*, vol. 20, no. 3, pp. 507–514, 2002.

[8] X. Zhao, J. Kivinen, P. Vainikainen, and K. Skog, "Characterization of doppler spectra for mobile communications at 5.3 GHz," *IEEE Transactions on Vehicular Technology*, vol. 52, no. 1, pp. 14–23, 2003.

[9] L. Cheng, B. E. Henty, D. D. Stancil, F. Bai, and P. Mudalige, "Mobile vehicle-to-vehicle narrow-band channel measurement and characterization of the 5.9 GHz Dedicated Short Range Communication (DSRC) frequency band," *IEEE Journal on Selected Areas in Communications*, vol. 25, no. 8, pp. 1501–1516, 2007.

[10] C. Lin, E. H. Benjamin, D. S. Daniel, and B. Fan, "Doppler component analysis of the suburban vehicle-to-vehicle DSRC propagation channel at 5.9 GHz," in *Proceedings of IEEE Radio and Wireless Symposium (RWS '08)*, pp. 343–346, January 2008.

[11] I. Tan, W. Tang, K. Laberteaux, and A. Bahai, "Measurement and analysis of wireless channel impairments in DSRC vehicular communications," in *Proceedings of IEEE International Conference on Communications (ICC '08)*, pp. 4882–4888, May 2008.

[12] D. C. Cox, "Delay Doppler characteristics of multipath propagation at 910 MHz in a suburban mobile radio environment," *IEEE Transactions on Antennas and Propagation*, vol. 20, no. 5, pp. 625–635, 1972.

[13] J. S. Davis and J. Linnartz, "Vehicle to vehicle RF propagation measurements," in *Proceedings of the 28th Asilomar Conference on Signals, Systems and Computers*, vol. 1, pp. 470–474, October 1994.

[14] D. Tse and P. Viswanath, *Fundamentals of Wireless Communication*, Cambridge University Press, New York, NY, USA, 1st edition, 2005.

[15] T. Rappaport, *Wireless Communications: Principles and Practice*, Prentice Hall, Englewood Cliffs, NJ, USA, 2nd edition, 2002.

[16] A. S. Akki and F. Haber, " A statistical model of mobile-to-mobile land communication channel," *IEEE Transactions on Vehicular Technology*, vol. 35, no. 1, pp. 2–7, 1986.

[17] A. Doufexi, S. Armour, M. Butler et al., "A comparison of the HIPERLAN/2 and IEEE 802.11a wireless LAN standards," *IEEE Communications Magazine*, vol. 40, no. 5, pp. 172–180, 2002.

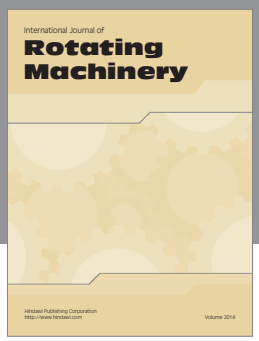

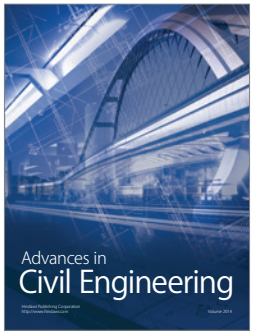

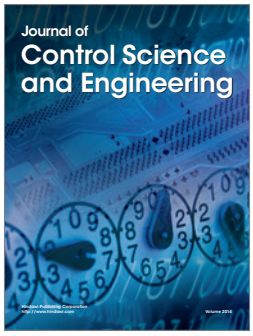

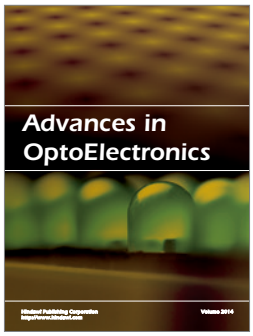

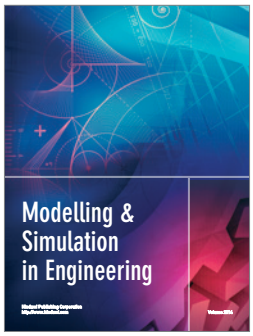

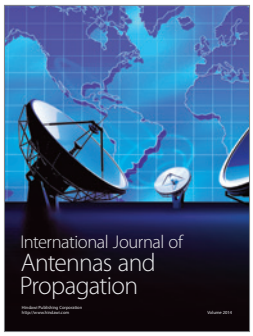

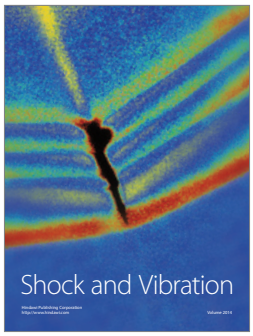

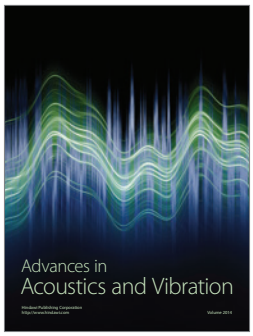

Hindawi

Submit your manuscripts at
http://www.hindawi.com